THE JOURNAL OF COMPARATIVE NEUROLOGY 510:145–157 (2008)

Spatiotemporal Distribution of Proteoglycans in the Developing Rat's Barrel Field and the Effects of Early Deafferentation

CARLOMAGNO PACHECO BAHIA,[1,2] JEAN-CHRISTOPHE HOUZEL,[2] CRISTOVAM WANDERLEY PICANÇO-DINIZ,[1] AND ANTONIO PEREIRA JR[1]*
[1]Institute of Biological Sciences, Universidade Federal do Pará, 66075-900 Belém, PA, Brazil
[2]Department of Anatomy, ICB, Universidade Federal do Rio de Janeiro, 21491-590 Rio de Janeiro, RJ, Brazil

ABSTRACT

The isolectin *Vicia villosa* B_4 (VV) selectively recognizes *N*-acetyl-galactosamine-terminal glycoconjugates that form perineuronal nets (PNNs) around a subset of neurons in the cerebral cortex. PNNs are thought to participate in the guidance of incoming thalamic axons and in the posterior stabilization and maintenance of synaptic contacts. Here we examine the spatial and temporal distribution of biotinylated VV in tangential sections through layer IV of the posteromedial barrel subfield in the primary somatosensory cortex (PMBSF) of rats ranging from postnatal day (P)3 to P60, which underwent unilateral deafferentation of whiskers at birth. In the afferented hemisphere, labeling first appears at P5, with a diffuse distribution, probably associated with neuropil, inside PMBSF barrels. VV distribution remains diffuse during the following week, and declines around P17. From P24 onward, however, proteoglycans form PNNs around cell bodies preferentially localized in septal regions of the PMBSF. In the contralateral, deafferented PMBSF the diffuse labeling also appears on P5, but first develops into elongated, homogeneous stripes, which disappear after P24, leaving only scattered cell bodies along layer IV. Our results indicate that proteoglycans appear simultaneous to barrel formation in the developing rat while segregation of PNNs to septal cells might be driven by afferent activity. J. Comp. Neurol. 510:145–157, 2008.

Indexing terms: proteoglycans; extracellular matrix; perineuronal net; plasticity; critical period; somatosensory cortex

The primary somatosensory cortex (Area S1) of mammals contains an orderly representation of the body surface that privileges behaviorally important parts. In rats and mice, for instance, the somatotopic map in S1 is dominated by face inputs, particularly from the large mystacial vibrissae (whiskers), which are individually represented by modules in the posteromedial barrel subfield, PMBSF (Woolsey and Van der Loos, 1970; Welker and Woolsey, 1974; Welker, 1976; Welker and Van der Loos, 1986; Petersen, 2007). The isomorphic relationship between individual whiskers and cortical barrels is an ideal model to study the developmental plasticity of thalamocortical projections (Daw et al., 2007). Barrels can be easily visualized with several histological procedures, such as the Nissl stain (Woolsey and Van der Loos, 1970), or by revealing the activity of enzymes such as cytochrome oxidase (Wong-Riley and Welt, 1980; Land and Simons, 1985), succinate dehydrogenase (Dawson and Killackey, 1987; Wallace, 1987), or nicotinamide adenine dinucleotide phosphate-diaphorase (NADPH-d) (Pereira et al., 2000). Barrels begin to form around postnatal day (P)4 in rats, simultaneous with the arrival of thalamic afferents

*Correspondence to: Dr. Antonio Pereira, Universidade Federal do Pará, Centro de Ciências Biológicas, 66075-900, Belém (PA), Brazil.
E-mail: apereira@ufpa.br

Received 29 December 2006; Revised 19 April 2008; Accepted 9 May 2008
DOI 10.1002/cne.21781
Published online in Wiley InterScience (www.interscience.wiley.com).

to the differentiating layer IV (Rice, 1985, 1995; Rice et al., 1985), and early manipulation of the sensory periphery can profoundly alter the PMBSF normal layout (reviewed in Inan and Crair, 2007). Much progress has been made toward unraveling the cellular and molecular interactions responsible for guiding thalamic axons to their final destination in the PMBSF, and eventually promote synaptic stabilization (Bender et al., 2006; Inan et al., 2006; Uziel et al., 2006). However, the precise developmental mechanisms responsible for defining barrel domains are still nuclear.

The extracellular matrix (EM) of the brain is a rich source of a class of macromolecules known as proteoglycans, which are composed of glycosaminoglycan chains covalently bound to a protein core (Cooper and Steindler, 1986b; Ruoslahti, 1996; Rauch, 1997; John et al., 2006). Perineuronal nets (PNNs) are a specialized form of the EM that were first described by Camillo Golgi in the 19th century (for review, see Celio et al., 1998). PNNs are particularly rich in a class of macromolecules known as chondroitin sulfate proteoglycans (Herndon and Lander, 1990), proteins that have one or more glycosaminoglycan sidechains. Brevican, for instance, is one of the most prominent constituents of the EM during postnatal development of the rodent brain (see Yamaguchi, 2000). In vitro assays revealed that brevican is primarily synthesized by co-cultured astrocytes and coalesces, with other proteoglycans, onto PNNs around neuronal somata and processes (John et al., 2006). Brevican is synthesized relatively late during ontogenetic development, in a period coinciding with synaptogenesis and the final stages of brain wiring (Seidenbecher et al., 1995; Seidenbecher et al., 1998). The relative composition of PNNs depends on neuronal type, cerebral region, or even the species under consideration (review in Deepa et al., 2006). For instance, PNNs are mainly found around some parvalbumin-immunoreactive inhibitory neurons in the cerebral cortex of rodents (Celio and Chiquet-Ehrismann, 1993; Celio and Blumcke, 1994; Elston et al., 1999; Viggiano, 2000; but see Ojima et al., 1995; Alpar et al., 2006), whereas they can be found on pyramidal cells in both the marsupial and primate cortex (Hausen et al., 1996; Bruckner et al., 1998). In all cases, PNNs form coatings around somata, defining microenvironments which extend to proximal dendrites and initial segment of axons. PNNs are supposed to be involved in various aspects of neuronal function, such as axon-guidance, concentration of growth factors around select neurons, maintenance of intercellular relationships and synapse stabilization, integration of synaptic inputs, and establishment of the electrical properties of cell membranes (Hendry et al., 1988; Mulligan et al., 1989; Celio et al., 1998; Beneyto et al., 1999; Viggiano, 2000; Bruckner et al., 2006). Indeed, the postnatal development of PNNs coincides with key periods of axonal growth, synaptic refinement, maturation of voltage-gated ionic channels, myelination, and with the establishment of adult-like patterns of neuronal activity (Wintergerst et al., 1996; Koppe et al., 1997; Ohyama and Ojima, 1997). Recent studies have shown that disrupting PNN integrity can influence not only development, but also plasticity and regeneration in the adult central nervous system (Pizzorusso et al., 2002; Dityatev and Schachner, 2003; Pizzorusso et al., 2006; Massey et al., 2006; Kaas et al., 2008).

Plant lectins such as *Vicia villosa, Wisteria floribunda* agglutinin (WFA), *Dolichos biflorus* and *Glycine max*, have successfully been used to reveal PNNs in rats (Bruckner et al., 1996), opossums (Bruckner et al., 1998), mice (Hartig et al., 1992; Bruckner et al., 2003; McRae et al., 2007), gerbils (Bruckner et al., 1994), guinea pigs (Ohyama and Ojima, 1997), humans (Bertolotto et al., 1990), and New World monkeys and agoutis (Picanço-Diniz et al., unpubl. results). The isolectin *Vicia villosa* agglutinin B_4 (VV) used in the present study is a 35,900 kD molecule that recognizes *N*-acetyl-*d*-galactosamine residues linked to serine or threonine in glycoconjugates (Tollefsen and Kornfeld, 1983, 1987). It was initially reported that in the cerebral cortex VV is associated with a subpopulation of parvalbumin-immunoreactive GABAergic interneurons, in a way similar to WFA (Kosaka and Heizmann, 1989). However, more recently PNNs labeled with VV were found both in pyramidal and nonpyramidal neurons in the guinea pig (Ojima et al., 1995; Ohyama and Ojima, 1997), and rat cortex (Alpar et al., 2006). These latter findings reinforce the notion that both lectins might label similar neurons. VV and WFA are also associated with a layer-specific pattern of diffuse neuropil labeling in the cortex (Derouiche et al., 1996).

Here we examine the labeling pattern of biotinylated VV bound to proteoglycans in tangential sections of the developing rat's S1. We paid close attention to the postnatal period corresponding to the formation and maturation of the thalamo-recipient layer IV in the PMBSF. To assess the influence of peripheral inputs on VV-distribution, animals underwent neonatal deafferentation of all principal whiskers located on one side of the face. The results demonstrate that, whereas the spatiotemporal pattern of VV distribution display a close similarity to the PMBSF layout during normal postnatal development, early whisker removal disrupts both the establishment of the VV-binding pattern and the formation of the barrel field.

Abbreviations

ANOVA	Analysis of variance
CO	Cytochrome oxidase
EM	Extracellular matrix
GABA	γ-amino butyric acid
GFAP	Glial fibrillary acidic protein
PMBSF	Posteromedial barrel subfield
PNN	Perineuronal net
SE	Standard error
VV	*Vicia villosa* B_4 isolectin
VV^+	*Vicia villosa*-positive cell

MATERIALS AND METHODS

Experimental animals

Wistar rat pups (n = 28) were obtained from the Central Animal Facility at Universidade Federal do Pará. Experimental procedures followed the "Guide for the Care and Use of Laboratory Animals" (NIH publication, No. 86-23, revised 1985) and all efforts were made to avoid animal suffering and to reduce the number of animals used. On the day of birth (P0), all animals were deeply anesthetized by hypothermia and all whiskers on the right snout were removed by cauterization. Twenty-eight animals of different postnatal ages (P3, P5, P10, P17, P24, P32, and P60) were deeply anesthetized with a mixture of xylazine (Rompun, Bayer, Leverkusen, Germany; 25 mg/kg, i.m.)

and ketamine chloride (Ketalar, Parker-Davis, Detroit, MI; 100 mg/kg, i.m.) and subsequently perfused transcardially with saline phosphate buffer (PB, pH 7.4, 0.1M) followed by 4% paraformaldehyde in PB. The cerebral hemispheres were removed from the skull, flattened overnight between two glass slides, immersed in PB at 4°C, and cut tangentially with a vibratome (Pelco 1000) into serial, 50 μm-thick sections.

Histochemistry for cytochrome-oxidase and *Vicia villosa*

For one animal of each age group (14 hemispheres), sections were processed alternately to reveal either cytochrome oxidase (CO) activity or biotinylated VV bound to proteoglycans. For revelation of CO, sections were incubated in a solution containing 0.03% cytochrome-C (Sigma, St. Louis, MO), 0.02% catalase (Sigma), and 0.05% diaminobenzidine (Sigma) in 0.1 M PB (Wong-Riley, 1979). Development of the CO reaction was monitored regularly under microscopic observation and interrupted when the signal/background level was deemed satisfactory.

The remaining sections from these 14 hemispheres and all sections from the other 42 flattened hemispheres were processed to reveal specific glycosaminoglycans by way of their affinity to the *V. villosa* lectin. Sections were first incubated for 16–24 hours at 20°C in PB containing 0.5% biotinylated VV (Vector, Burlingame, CA) and 6% Triton X-100 (Sigma). Control sections were incubated only in PB without the lectin. After three washes in PBS, all sections were incubated in avidin-biotin-peroxidase complex (ABC, 1:200; Vector) and the peroxidase was revealed using the diaminobenzidine reaction intensified with nickel ammonium sulfate (Shu et al., 1988). Finally, sections were mounted onto gelatin-coated glass slides, dehydrated, and coverslipped with Entellan (Merck, Germany).

Electrophysiological recordings

Multiunit electrophysiological responses to peripheral tactile stimulation were recorded bilaterally in the PMBSF of two P32 and two P60 animals. In each case the principal whiskers of the right snout had been surgically removed at P0. The day before the recording sessions, animals were given dexamethasone (Decadron, Prodome, Sao Paolo, Brazil; 1.0 mg/kg, i.m.) and vitamin K (Kanakion, Roche, Nutley, NJ; 1.0 mg/kg, i.m.) to prevent brain edema and excessive bleeding, respectively. For surgery, anesthesia was induced with a mixture of xylazine (4 mg/kg) and ketamine chloride (46 mg/kg), additional doses being subsequently administered as necessary. Body temperature was maintained at about 37°C with a heating pad. The head of the animal was secured in a stereotaxic apparatus and the skull overlying the parietal cortex was partially removed with a dental drill. The exposed brain was protected with agar and a digital picture of the blood vessel pattern was taken to mark the location of microelectrode penetrations.

Multiunit signals from tungsten microelectrodes (9–12 MΩ at 1 kHz, FHC, Bowdoinham, ME) were amplified, bandpass-filtered between 1 and 3 kHz (ME04011, FHC), and fed simultaneously to an oscilloscope (1476A, BK Precision, Yorba Linda, CA) and an audio monitor (SR771, Sansui, Japan). Responses to mechanical stimulation of single vibrissa or to light taps of the skin were characterized and the corresponding receptive fields were plotted. At the end of the recording session, electrolytic lesions were made by passing positive current through the microelectrode (10 μA, 10 sec, 52413 Precision Current Source, Stoelting, Wood Dale, IL) to allow the subsequent alignment of the recording sites with the histological sections. The animal was then given an overdose of anesthetics and perfused transcardially with PBS followed by 4% paraformaldehyde.

Quantitative analysis of *V. villosa*-labeled neurons in the PMBSF

Serial sections were observed with a Zeiss Axioplan microscope; low- and high-power microphotographs were taken using an Axiocam digital camera (HR series, Zeiss, Germany) with the Axiovision software (Zeiss). All tangential sections through PMBSF's layer IV were reconstructed with a light microscope (Nikon Optiphot-2, Japan) equipped with a high-resolution micromonitor (Lucivid, MBF Bioscience, Williston, VT) attached to the drawing tube and a 3D-motorized stage (MAC5000, Ludl, Hawthorne, NY). All devices were connected to a PC running the Neurolucida software (MBF Bioscience). First, the 14 hemispheres whose sections were alternately processed to reveal CO activity were analyzed: outlines of the CO-stained sections, of some blood vessels, and of all CO-rich domains within the parietal cortex were drawn. Alternate VV sections were also drawn and all positive (VV^+) neurons were plotted under direct microscopic examination at 20× magnification. Using both the sections' contours and the blood vessel pattern as fiduciary marks, reconstructions of consecutive CO- and VV-reacted sections were precisely aligned and each VV^+ neuron could be identified with a marker as belonging either to barrels or septa (see Fig. 1). Since the distribution of VV labeling (both diffuse and pericellular, see Results) proved to match very closely the contours of CO-rich PMBSF domains in layer IV at all ages, subsequent hemispheres were processed only for VV, so that all VV^+ neurons located in layer IV were plotted in consecutive sections. Depending on the animal's age, layer IV contained four to six 50-μm-thick tangential sections. All cells with clear profiles were counted in each PMBSF compartment (septa and barrels) at every postnatal age (P24, P32, and P60). In afferented hemispheres we counted every positive cell within layer IV of the entire PMBSF area. In the deafferented hemispheres, cells were counted within a region identical, both in surface area and location (relative to other S1 compartments) to the reconstructed PMBSF in the opposite, normal hemisphere. The density of VV^+ cells inside barrels and septa was computed for all postnatal groups using the NeuroExplorer software (MBF Bioscience). Average values for barrels and septa, expressed as MEAN ± SE, were compared using the two-tailed Student's *t*-test. Numbers of VV^+ cells within the PMBSF were compared across different groups using analysis of variance (ANOVA) and the Tukey post-hoc test, with $\alpha = 0.05$.

Eventual changes in cell diameter in the PMBSF compartments due to deafferentation and postnatal maturation could require the use of a correction factor to compensate for the resulting overestimation of cell numbers (Guillery and Herrup, 1997; Guillery, 2002). Thus, for each compartment and age group (see Table 1) we mea-

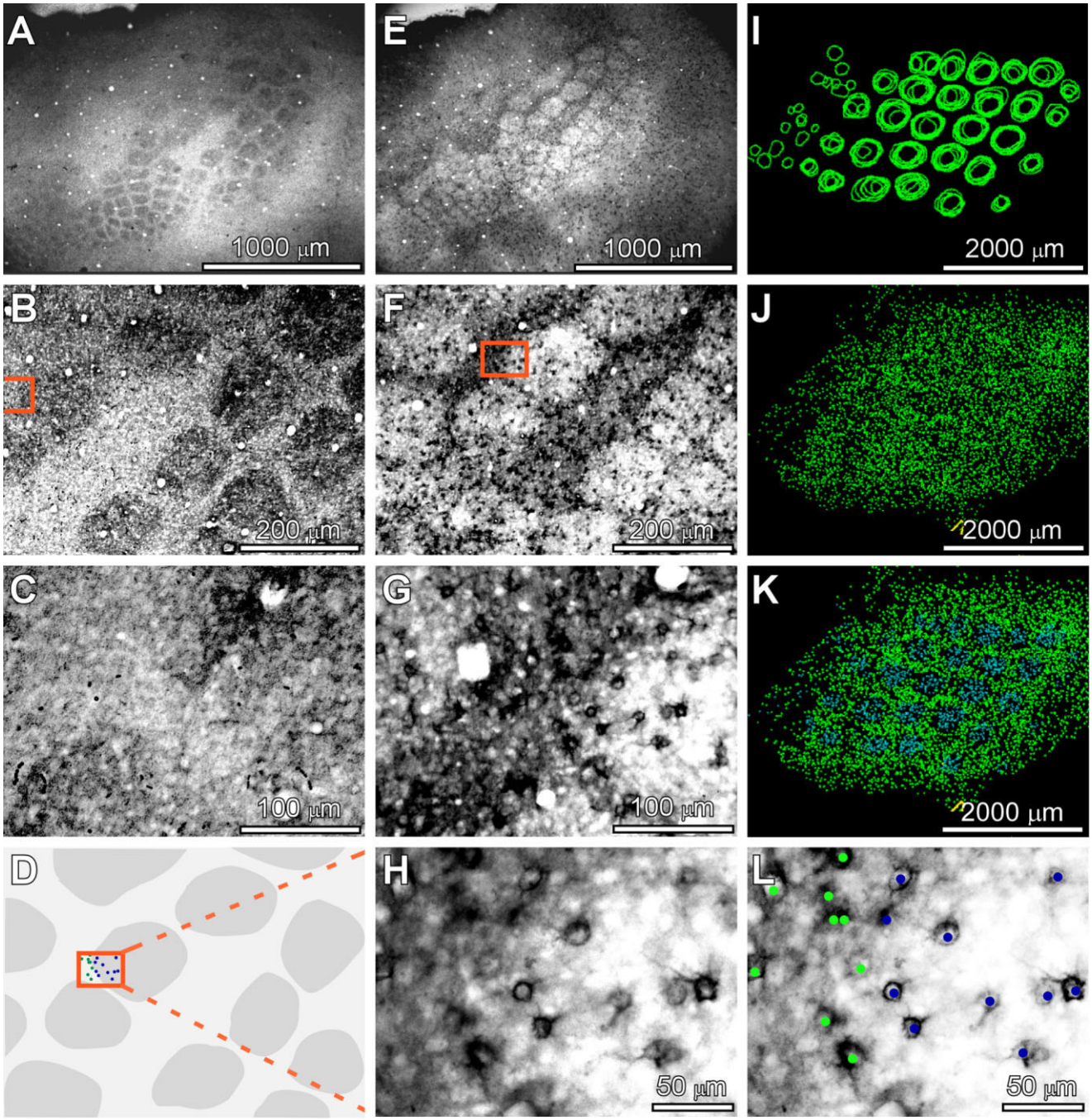

Fig. 1. Plotting *Vicia villosa* cells in tangential sections. Photomicrographs taken at increasing magnification from two consecutive, 50-μm-thick tangential sections of the afferented PMBSF of a P60 rat stained for CO **(A–D)** and *Vicia villosa* **(E–H,L)**. Note that at this age, the distribution of VV labeling (E) looks like a negative image of the CO activity pattern. The series of CO-stained sections passing through layer IV was used to determine, using a 5× objective, the limits of barrels and septa (respectively dark and light gray in D). Using higher-power objectives, all VV^+ cells were plotted from the alternate series of sections. Individually digitized sections were then merged and aligned using fiducial landmarks with the help of the Neurolucida system. After alignment, each VV^+ cell **(J)** was assigned a code according to its position: in **(K)**, cells within barrels and septa are represented by blue and green dots, respectively. H and L show the area corresponding to the box in D.

sured the diameter of 30 randomly selected VV+ cells. The measurements were made using a 100× objective and a high-resolution Axiocam digital camera (Zeiss) with the help of the Axiovision software (Zeiss). Average values were compared by a three-way repeated-measure ANOVA with the following factors: compartment (barrel, septum), postnatal age (P24, P32, P60), and hemisphere (afferented, deafferented). We found no significant difference in

cell diameter between different ages and concluded that in our sample the diameter of labeled cells did not significantly change following deafferentation and postnatal maturation in any PMBSF compartment (Table 1, Fig. 2). We presented data as cell density (number of cells/mm^3) and used an Abercrombie correction factor (Abercrombie, 1946) calculated for each compartment of the deafferented and deafferented hemisphere at all ages examined (Table 1). As additional measures to minimize the incidence of errors, the criteria to define regions and objects of interest were confirmed by at least two independent observers and all brains were fixed, cut, stained, and counted using the same protocols (Howard and Reed, 2005).

For data presentation, alterations to the images were limited only to global contrast and brightness adjustments using Adobe Photoshop CS (Adobe Systems, San Jose, CA). Additionally, images were cropped and mounted onto figure panels using the ACDsee Canvas 11 software (ACD Systems International, Victoria, Canada).

TABLE 1. Diameter of VV$^+$ Cells in Normal and Deafferented PMBSF Subcompartments of Postnatal Rats

				Diameter of VV+ cells (μm)					
				Afferented hemispheres				Deafferented hemispheres	
		Number of hemispheres processed		Barrels		Septa		PMBSF	
Age	Number of animals	Afferented	Deafferented	(Mean ± SE)	Abercrombie factor	(Mean ± SE)	Abercrombie factor	(Mean ± SE)	Abercrombie factor
>P24	3	3 (30 cells)	3 (30 cells)	15.04 ± 1.004	0.769	15.04 ± 0.993	0.769	14.04 ± 0.959	0.781
P32	3	3 (30 cells)	3 (30 cells)	14.14 ± 0.963	0.780	14.37 ± 0.975	0.777	14.60 ± 0.985	0.774
P60	3	3 (30 cells)	3 (30 cells)	14.41 ± 0.356	0.776	15.12 ± 0.321	0.768	14.94 ± 0.338	0.770
Total	9	9	9	90 cells		90 cells		90 cells	

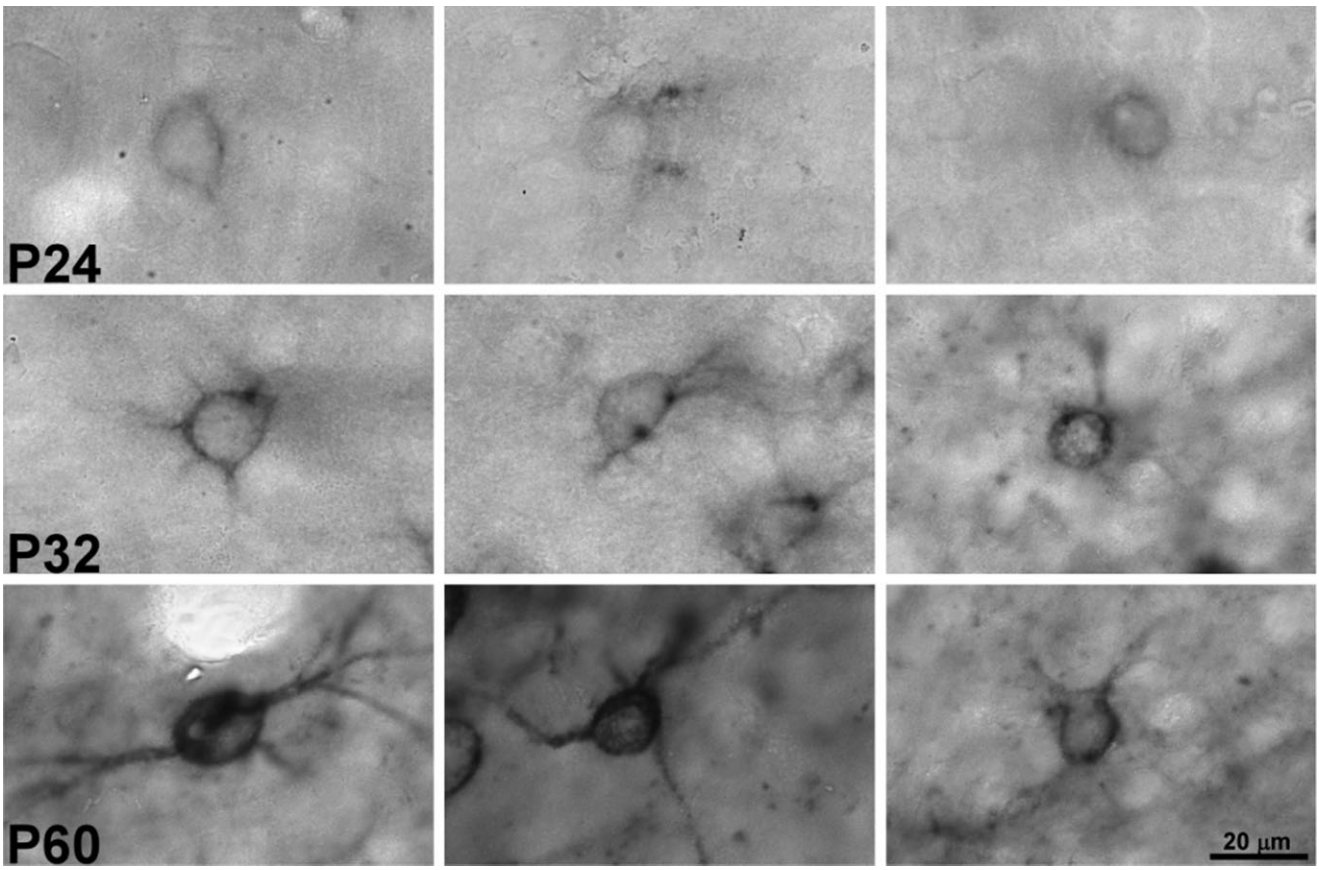

Fig. 2. The diameter of *Vicia villosa* labeled neurons. High-power photomicrographs of representative layer IV cells from different age groups (P24, P32, P60), different PMBSF compartments (barrel and septa: left and center columns, respectively), and afferented (left and center columns) and deafferented (right column) hemispheres. Note that although PNNs become denser during maturation, the diameter of cell profiles does not change across the age groups studied, nor does it depend on localization within the PMBSF or on the presence of peripheral inputs.

RESULTS

Development of *V. villosa* labeling in the PMBSF

No VV labeling could be detected in the PMBSF of P3 rat pups. VV labeling was first evident at P5 in tangential sections through layer IV and revealed the characteristic PMBSF modularity by way of diffusely stained patches clearly separated by regions of weaker intensity (Fig. 3). During the first 2 postnatal weeks, the PMBSF intrinsic organization revealed by VV closely matched the CO reactivity pattern (compare Fig. 4A,A′). The similarity of both labeling patterns was remarkable, especially at low magnification (Fig. 4). In the hemispheres of P17 rats, the diffuse VV labeling was still present, although markedly reduced (see Figs. 3, P17, and 4C,C′). In short, the first 3 postnatal weeks were characterized by a rather diffuse VV labeling with no discernible pericellular coatings, and by a preferential labeling of barrel centers as compared to septal regions.

From P24 onward the labeling pattern was conspicuously different. At low magnifications, for instance, the aspect of VV labeling in tangential sections through layer IV was virtually a negative image of the pattern described above for younger animals, since VV was now concentrated in septa, while barrels were weakly stained. At increasing magnification, it was clear that the labeling was not diffusely associated with neuropil as before, but rather concentrated around some cells, forming pericellular coatings typical of PNNs (Fig. 3). The latter pattern is more characteristic of perineuronal nets and has been previously described with several immunocytochemical and ultrastructural techniques in diverse cerebral regions (see Introduction). In the analysis below, VV^+ cells refers to the subpopulation of cells with evident pericellular VV coatings. In younger rats (P24, see Fig. 3), the coatings around some cells were punctated, suggesting that immature PNNs contain less compact aggregates of VV-binding material that become stronger as the animal matures.

Quantitative analysis

Since localization of the VV labeling appeared to have shifted from one PMBSF compartment to the other around the third postnatal week, we investigated the spatial relationship between barrels (defined both histochemically and electrophysiologically) and VV^+ cells. Standard extracellular microelectrode recordings were performed in two P32 and two P60 non-deafferented hemispheres. In agreement with previous reports (Welker, 1971, 1976), the cortical location of sites responsive to mechanical stimulation of the vibrissae was consistent with the topographically ordered tangential arrangement of CO-rich domains in the PMBSF (Fig. 5). In all these four hemispheres and two additional P24 normal hemispheres, alternate tangential sections were processed for CO and VV histochemistry. The same procedure was followed for pups from P5 to P17. The contours of CO-rich modules were serially reconstructed and the location of all VV^+ cells was independently plotted (Fig. 5). Subsequent alignment of both sets of sections with the Neurolucida software indicated that the vast majority of VV^+ cells were actually located within septa (see Fig. 1). Furthermore, since VV^+ cells were densely packed within septa, this compartment displayed a strong background reactivity, which contrasted with barrels (Fig. 4B,B′). Indeed, the contours of regions with high VV background could be precisely superimposed on the contours of CO poor regions, and were actually sufficient to determine whether any given cell was located within a barrel or a septum. Since PMBSF septa could be identified by the stronger background staining, allowing the same accuracy as obtained with CO sections (see Fig. 1), all sections from the remaining 48 hemispheres were processed for VV only, so that all VV^+ cells in layer IV could be plotted. Depending on the age of the animal, layer IV was completely contained within 4–6 consecutive 50-μm-thick sections, all of which were used for quantification.

Quantitative analysis (Fig. 6) revealed a progressive and significant increase ($P < 0.05$, ANOVA with Tukey post-hoc test) in the density (cells/mm^3) of VV^+ cells within layer IV (P24 = 1,930 ± 137, P32 = 3,283 ± 90, and P60 = 5,576 ± 439). The density of VV^+ cells increased by a factor of 2.8 between P24 and P60. Since the PMBSF area does not increase significantly after the fourth postnatal week in rats (Freire et al., 2004), this indicates a genuine increase of cellular elements with mature PNNs. Although VV^+ cell density increased in both compartments of the PMBSF, the density of VV^+ cells located within barrels (P24 = 1,123 ± 209; P32 = 1,150 ± 108; P60 = 3,422 ± 185) was significantly lower ($P < 0.05$, Student's *t*-test) than those located within septa (P24 = 2,556 ± 131; P32 = 5,391 ± 138; P60 = 7,508 ± 767) at all ages within layer IV (Fig. 6). Our results indicate that whereas the earliest PNNs can be identified around PMBSF neurons of P24 rats, their numbers keep increasing during maturation of the brain.

Effect of early vibrissae removal on VV labeling

Since proteoglycans first appear diffusely within barrels at P5, while PNNs develop preferentially within septa during a relatively extended postnatal period, we investigated the effects of peripheral deafferentation on the spatiotemporal distribution of VV-labeling (Fig. 6). This was assessed in the same animals by direct comparison of VV and CO reactivity patterns between the right, afferented hemisphere, and the left, deafferented hemisphere in 28 rats (age P3–P60) whose whiskers had been cauterized on the right side of the face at P0. Removal of facial whiskers at birth precluded the formation of the normal VV pattern in the affected hemisphere, also preventing, as expected, the formation of the normal pattern of CO tangential arrangement reactivity in the PMBSF (Figs. 4, 5). Instead of the typical arrangement of barrels in lines and columns, we observed elongated stripes of CO activity in layer IV of the deprived hemisphere at all studied ages (Fig. 4C′). A similar disruption was observed in the deafferented hemispheres of P5, P10, and P17 animals, with elongated bands of diffuse VV labeling replacing the normal PMBSF pattern (Fig 4C). However, although CO stripes could still be seen after P24, the bands of diffuse VV label disappeared by the third postnatal week. After this stage a few cells displayed typical PNNs, but they were randomly scattered across the tangential extent of layer IV, without any evident spatial organization (Figs. 4D, 5). Although the density of VV+ cells remained the same during the maturation of the deafferented PMBSF (P24 = 1,020 ± 50; P32 = 1,212 ± 12; P60 = 1,265 ± 63) ($P > 0.05$), it was significantly lower than the values found in the afferented PMBSF in every age analyzed ($P < 0.01$, and see Fig. 6).

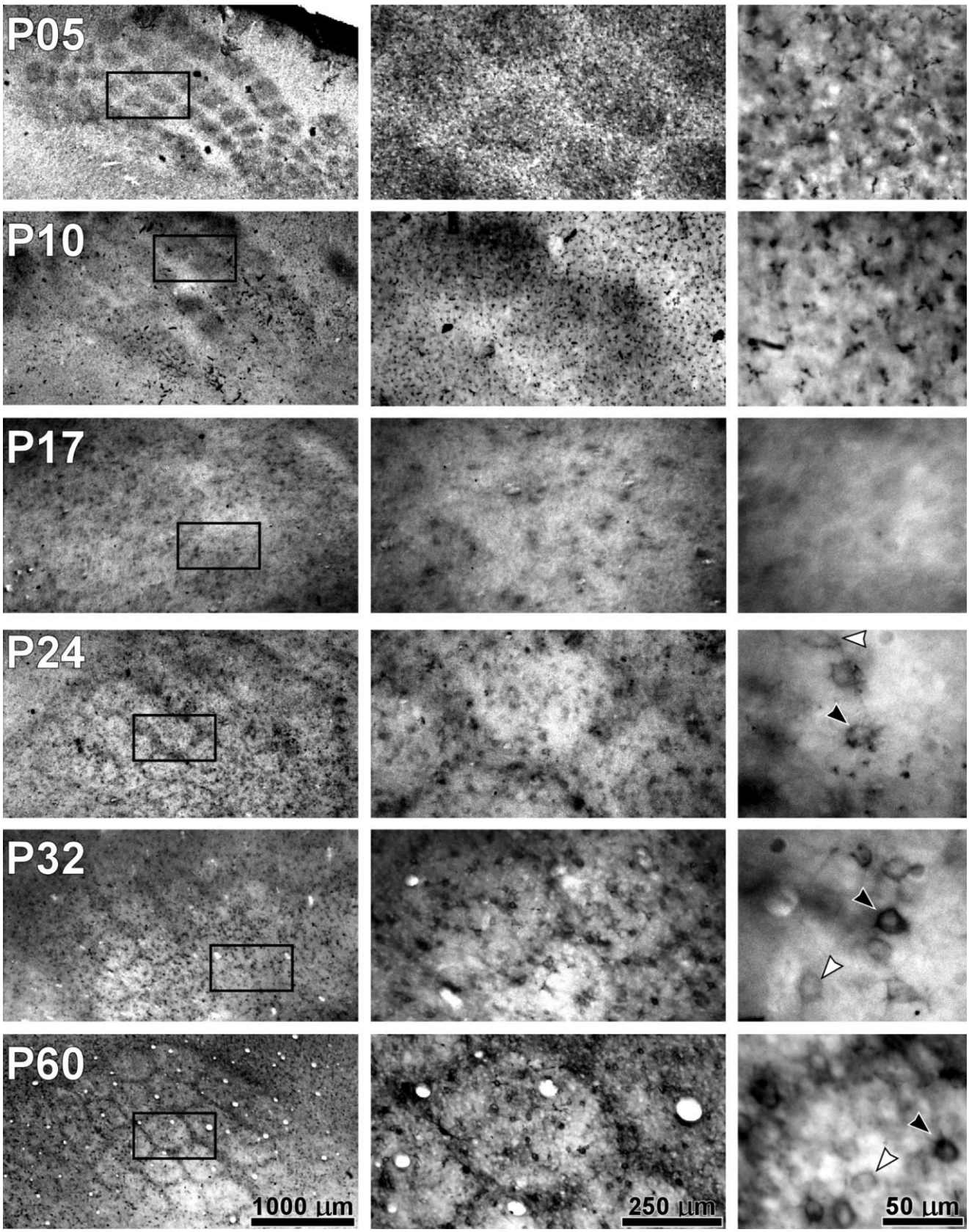

Fig. 3. *Vicia villosa* labeling during postnatal development of the PMBSF. Photomicrographs showing representative 50-µm-thick tangential sections through layer IV from P5 to P60. From P5 to P17, labeling is diffuse and more intense within barrels. At higher magnifications (center and right columns), reaction product can be seen dispersed through neuropil. From P24 onward labeling is concentrated around the soma of cells preferentially located within septa. Strongly (black arrowhead) and faintly (white arrowhead) labeled cells can be distinguished.

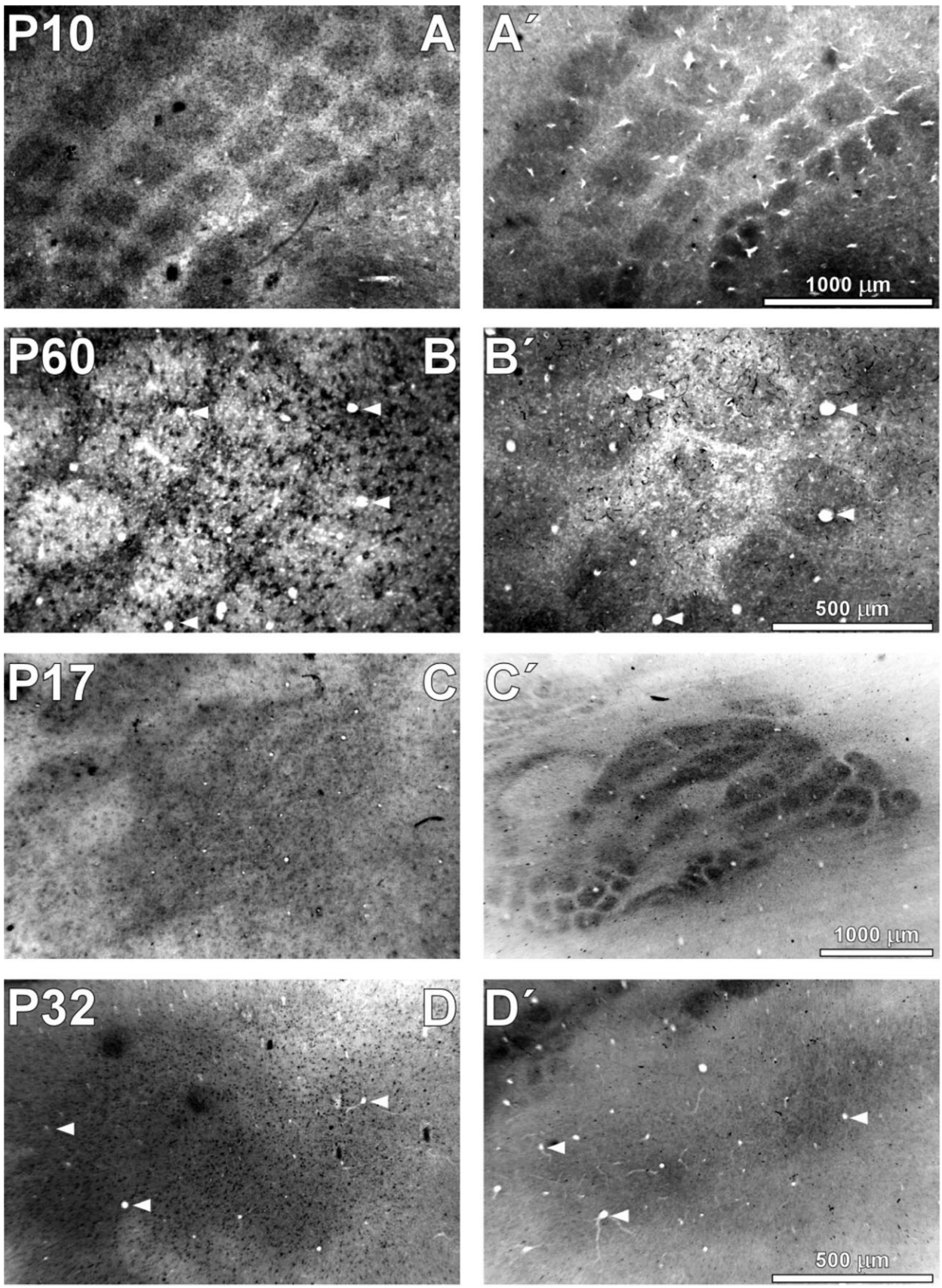

Fig. 4. Tangential pattern of *Vicia villosa* (left) and cytochrome oxidase (right) labeling in alternate sections through layer IV of normal **(A,A′,B,B′)** and whisker-deafferented **(C,C′,D,D′)** hemispheres during postnatal development. White arrowheads point to blood vessels used for section alignment. In afferented hemispheres, VV labeling closely matches the CO pattern in younger animals (first row, from top), whereas in adults (second row) they look like negative images of each other, since VV^+ cells appear preferentially in CO-poor septa. In deafferented hemispheres the typical barrel layout is completely disrupted from the beginning, although elongated CO-rich patches can still be distinguished (third and fourth row).

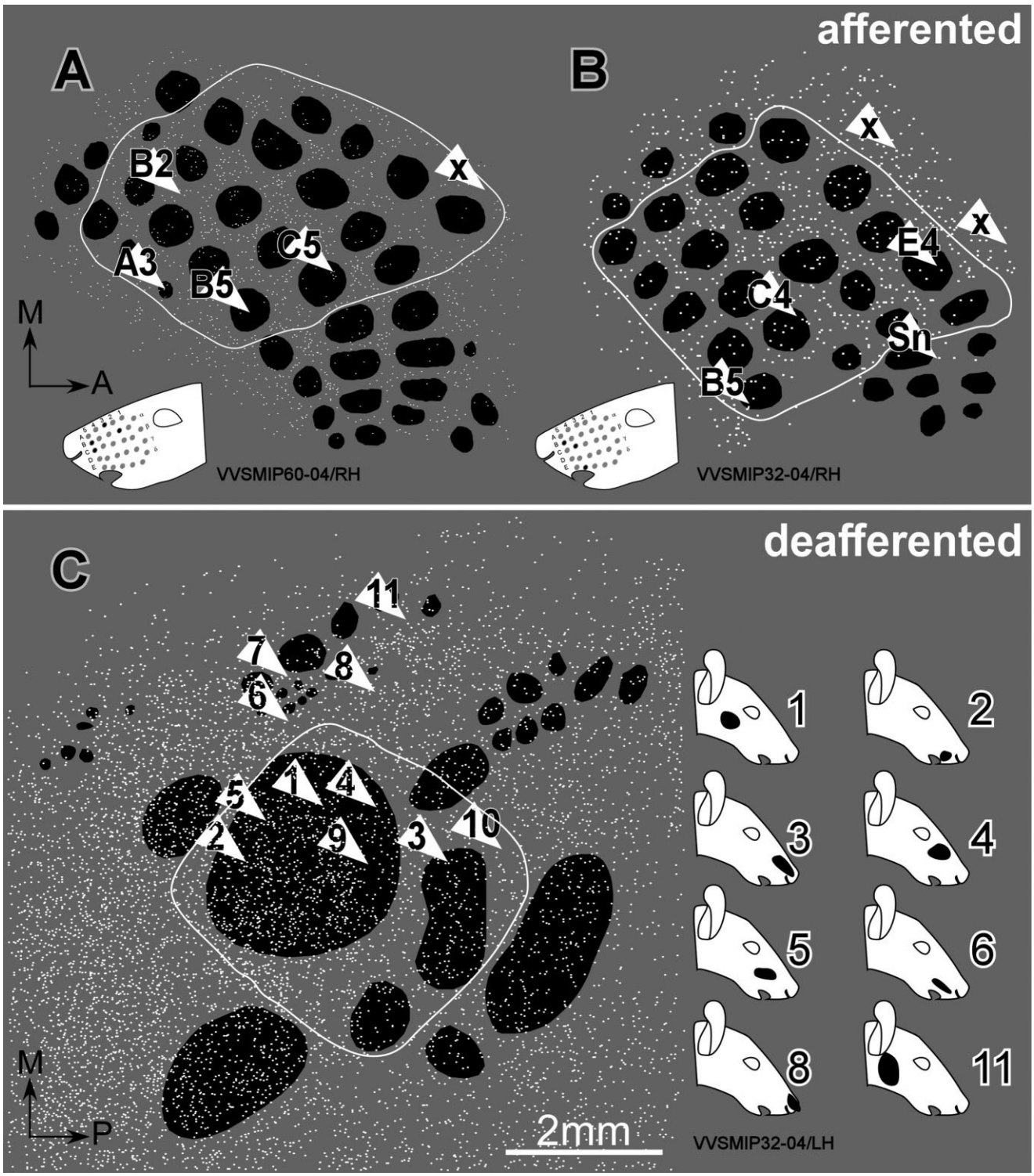

Fig. 5. Tangential reconstruction of the barrel field in afferented and deafferented hemispheres. For each case the illustration shows an overlay of the CO barrel pattern (black patches) with VV cells (VV^+, white dots), as serially reconstructed from alternate tangential sections through layer IV. **A:** Afferented hemisphere from a P60 rat (case VVSMIP60-04). **B,C:** Afferented and deafferented hemisphere, respectively, from a P32 rat (case VVSMIP32-04). Arrowheads indicate recording sites, with labels indicating the whisker eliciting the largest multiunit response in A,B; in C, numbers inside arrowheads indicate receptive field locations depicted on the right. The white line contour in A,B indicate the area used for cell counting. Note that the vast majority of VV^+ cells are located within septa. In C, the contour was transposed from the contralateral hemisphere from the same animal. Note that, in this case, deafferentation prevented the formation of the normal barrel pattern as well as the segregation of VV^+ cells into CO-poor domains.

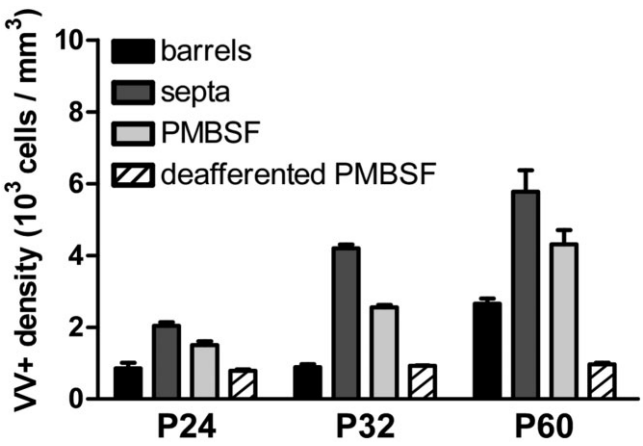

Fig. 6. Distribution of VV+ cells in PMBSF compartments during postnatal development of afferented and deafferented hemispheres. Values are expressed as average cell density ± SE (corrected by the Abercrombie factor; see Materials and Methods); data were obtained from three afferented hemispheres and three deafferented hemispheres for each age group (total: 32,388 cells). Black, dark gray, and light gray bars indicate, respectively, density of VV^+ cells located within barrels, septa, and the entire PMBSF in the afferented hemispheres. Note the significant and steady increase in cell density from P24 to P60 ($P < 0.05$, ANOVA/Tukey post-hoc test) for all compartments in the afferented hemisphere, with septa always having the greatest share ($P < 0.05$, Student's *t*-test). There were significant differences in the density of cells between the afferented and the deafferented PMBSFs in every age examined ($P < 0.05$, Student's *t*-test).

As expected, electrophysiological recordings from P32 and P60 deafferented hemispheres (Fig. 5C) confirmed that the somatotopic organization of sites responsive to light mechanical stimulation of the deafferented snout underwent a profound remodeling as a consequence of injury to the sensory periphery (e.g., Van der Loos and Woolsey, 1973; Rosen et al., 2001; Schierloh et al., 2004).

DISCUSSION

We analyzed, both qualitatively and quantitatively, the spatiotemporal distribution of PNN proteoglycans during maturation of the rat PMBSF. We were able to distinguish two successive stages of proteoglycan maturation in the PMBSF: during the first 2 weeks of life, VV-labeled proteoglycans show a diffuse, neuropil-associated distribution within barrels (diffuse stage). By the end of the third week, however, this pattern changes dramatically as labeling is heavily concentrated around the outer surface of cells, with the typical aspect of PNNs (pericellular stage). Besides, during this pericellular stage, PNN coated cells are located preferentially within septa, which now stand in contrast to the weakly stained barrel centers. This late pattern becomes even more evident during the following postnatal weeks, as the number of VV-labeled cells increases and the adult-like pattern is evident by the end of the first month in normal, whisker-afferented hemispheres. This is at odds with what has been reported for the mouse (Cooper and Steindler, 1986b). In that species the PMBSF delineation provided by the lectins concanavalin A, WGA, and peanut agglutinin (PA) is ephemeral, restricted to the first postnatal week (Cooper and Steindler, 1986b). Besides, even though the lectin-peroxidase reaction product is largely associated with neuropil in the first postnatal week, as in the rat, the reaction product is found *outside* barrel hollows, within sides and/or septa (Cooper and Steindler, 1986b). It has to be remembered, however, that PMBSF's cytoarchitecture is different in rats and mice: in mice the barrels are hollow, with the barrel sides displaying greater cell density, as shown with the cresyl violet stain. It is unclear how these cytoarchitectonic peculiarities relate to the differences observed in the lectin-peroxidase reaction pattern of the PMBSF of adult animals.

Our qualitative examination of VV-processed material confirms and extends previous observations by Koppe et al. (1997) showing that labeling for another lectin, WFA, which binds to *N*-acetyl-*d*-galactosamine, initially appears during the first postnatal week in the rat parietal cortex, then increases gradually during the following 2 weeks, after which many neurons become surrounded by clearly contoured, PNN-like, perisomatic coatings. In this study, immunostaining for chondroitin-sulfate proteoglycans yielded results that were largely identical to the lectin-binding patterns (Koppe et al., 1997).

The use of tangential sections through layer IV and alternate processing for CO activity further indicates that VV-binding compounds first accumulate in a pattern of diffuse neuropil staining within the PMBSF barrels before appearing in septa where they organize around cell bodies. In the early stages they form macroscopic boundaries, separating cells and molecules belonging to adjacent compartments, while later providing microscopic boundaries to segregate synaptic structures (Steindler, 1993). According to our results with whisker deafferentation, these changes in the spatiotemporal distribution of lectin-bound glycosaminoglycans might be due to experience-dependent modifications conveyed by the electrical activity of thalamocortical axons. This conclusion is consistent with the observation that diverse EM molecules such as tenascin (Steindler et al., 1989), cytotactin (Jhaveri et al., 1991), keratan (Geisert and Bidanset, 1993), and neurocan (Oohira et al., 1994; Watanabe et al., 1995) are locally downregulated within the barrels (Faissner and Steindler, 1995) during the critical period. The precise timing of proteoglycan expression seems to be specific to each particular cerebral region. In the rat olfactory bulb or the entorhinal cortex, for instance, lectin binding is already evident at birth and adult-like PNNs are found as early as P21 (Koppe et al., 1997). In the visual cortex of kittens, the soybean lectin labels neuropil only from the fourth to the seventh postnatal week, after which the typical pericellular coatings of PNNs can be seen (Schweizer et al., 1993).

In our study, mature VV coatings could first be seen around P24 and the number of VV^+ cells kept increasing from P32 to adulthood within PMBSF septa. The same observation holds true for NADPH-diaphorase cells (Freire et al., 2004). Both cell types seemingly constitute subgroups of GABAergic interneurons, which are preferentially located within septa and contribute to delineate a strong inhibitory zone surrounding the overwhelmingly excitatory thalamic input arriving in layer IV (Dawson and Killackey, 1985; Koralek et al., 1988). To what extent these two subpopulations share common elements has not yet been determined (Nakagawa et al., 1986). In light of recent studies demonstrating extensive networks of electrically coupled, parvalbumin-positive interneurons in the

visual cortex (Fukuda et al., 2006), the possibility that specific subpopulations of GABAergic interneurons form large networks extending across the barrel field should also be further investigated, in order to better understand the dynamics of inhibitory interactions between PMBSF sub compartments.

Specification of the tangential distribution of thalamocortical afferents in S1 is achieved in the early stages of forebrain development, as the lamination of cortex begins. During the first 2 postnatal weeks, activity-dependent mechanisms then become increasingly important to refine topographic maps, through elimination of exuberant axons and synapses (reviewed in Katz and Shatz, 1996; Innocenti and Price, 2005). In addition to thalamic fibers, callosal afferents also invade the cortical mantle during the early stages of postnatal development. Callosal axons arise primarily from septal neurons and terminate mainly in homotopic regions in the contralateral hemisphere (Olavarria et al., 1984; Ferezou et al., 2007). The spatial distribution of callosal afferents in S1 is therefore complementary to the thalamocortical layout and, since the former matures slightly later (Ivy et al., 1979), they are likely to be involved in the further restriction of the VV-labeled elements to septal domains. However, since callosal terminals tend to avoid layer IV, and since removal of thalamocortical inputs have dramatic effects on the VV-labeling patterns in layer IV, it is likely that the final layout results from the interplay between thalamocortical and corticocortical afferents.

The effects of early whisker removal on the VV-labeling pattern in the contralateral PMBSF are compatible with a number of earlier studies showing that the normal development of the barrel field depends on intact sensory inputs from the periphery (e.g., Van der Loos and Woolsey, 1973; Fuchs and Salazar, 1998). Our results show that in deafferented hemispheres, longitudinal stripes of diffuse VV-labeling could be seen during the first 2 postnatal weeks. The same pattern was observed in adjacent CO-labeled sections. Later on, at the time where PNNs could be detected around septal cells in the normal hemisphere (P24), the staining in the deafferented hemisphere was reduced to a few cells scattered in layer IV without any obvious regularity, even though CO-positive stripes could be seen well into adulthood. This result brings further support to the notion that the maturation of PNNs depends on specific patterns of neuronal activity. On the other hand, experiments using enzymatic digestion of chondroitin sulfate proteoglycans recently demonstrated that PNNs actually inhibit experience-dependent plastic modifications in the visual cortex occurring in the post-critical period (Pizzorusso et al., 2002, 2006), as well as sprouting in the caudate nucleus seen after spinal cord lesions (Massey et al., 2006; Galtrey and Fawcett, 2007; Kaas et al., 2008). Together with our present findings, these data suggest an exquisite interaction between peripheral activity and PNNs during development. Thus, even though the identity of somatosensory cortex is specified early during neurogenesis (Cohen-Tannoudji et al., 1994), finer architectural aspects are dependent on the interplay between intrinsic and extrinsic cues later during postnatal development. Recently, another work has shown that the normal development of PNNs in the mouse barrel cortex depends on peripheral tactile stimulation (McRae et al., 2007). The authors showed specifically that trimming the whiskers of newborn mice reduces the expression of the proteoglycan aggrecan in the PMBSF.

We hypothesize that proteoglycans labeled by VV lectin might be involved in at least two crucial stages in the establishment of the PMBSF intrinsic structure. In the initial phase, which extends from P5 to P17, proteoglycans associated with the immature neuropil, together with other EM molecules such as ephrins (review in Uziel et al., 2006), create microdomains in the barrels that are permissive to incoming thalamic afferents. The PMBSF parcellation provided by the lectin-peroxidase conjugates in the early postnatal mouse PMBSF (Cooper and Steindler, 1986b) (see above) is mirrored by the disposition of radial glia labeled with GFAP: on postnatal day 6, when the PMBSF is still barely visible in cresyl violet-stained tangential sections, the disposition of GFAP-positive radial glia around barrel hollows already shows the PMBSF pattern in its entirety, as reported by Cooper and Steindler (1986a). In adult mice, however, the authors show that GFAP antibodies label mature astrocytes that are more evenly distributed in the PMBSF, without a clear relationship to cytoarchitectonic compartments (Cooper and Steindler, 1986a). Our results show that in a second phase, extending from P24 onward, proteoglycans start to organize into PNNs around septal interneurons and form compartments that could be partly responsible for maintaining the recently formed connections and for the relatively limited plasticity seen in the mature PMBSF. This barrier function played by glycoconjugates in the PMBSF also occurs in the dorsal cochlear nucleus of the developing hamster (Riggs and Schweitzer, 1994), as PNA-delineated zones in the dorsal cochlear nucleus are effective in blocking the ingrowth of cochlear axons during development.

ACKNOWLEDGMENT

We thank Ms. Patricia Casale for helping in some experiments.

Financial support: PROCAD/CAPES 002401-5, PRONEX/FAPERJ E-26/171.210/2003, CNPq 411530/2003-8, 481132/2007-4, 479578/2006-0, and 304422/2006-1

LITERATURE CITED

Abercrombie M. 1946. Estimation of nuclear population from microtome sections. Anat Rec 94:239–247.

Alpar A, Gartner U, Hartig W, Bruckner G. 2006. Distribution of pyramidal cells associated with perineuronal nets in the neocortex of rat. Brain Res 1120:13–22.

Bender KJ, Allen CB, Bender VA, Feldman DE. 2006. Synaptic basis for whisker deprivation-induced synaptic depression in rat somatosensory cortex. J Neurosci 26:4155–4165.

Beneyto M, Rueda J, Merchan JA, Prieto JJ. 1999. Specific staining of nonpyramidal cell populations of the cerebral cortex by lectin cytochemistry on semithin sections. Brain Res Bull 49:251–262.

Bertolotto A, Rocca G, Schiffer D. 1990. Chondroitin 4-sulfate proteoglycan forms an extracellular network in human and rat central nervous system. J Neurol Sci 100:113–123.

Bruckner G, Seeger G, Brauer K, Hartig W, Kacza J, Bigl V. 1994. Cortical areas are revealed by distribution patterns of proteoglycan components and parvalbumin in the Mongolian gerbil and rat. Brain Res 658:67–86.

Bruckner G, Hartig W, Kacza J, Seeger J, Welt K, Brauer K. 1996. Extracellular matrix organization in various regions of rat brain grey matter. J Neurocytol 25:333–346.

Bruckner G, Hartig W, Seeger J, Rubsamen R, Reimer K, Brauer K. 1998. Cortical perineuronal nets in the gray short-tailed opossum (Monodel-

phis domestica): a distribution pattern contrasting with that shown in placental mammals. Anat Embryol (Berl) 197:249–262.

Bruckner G, Grosche J, Hartlage-Rubsamen M, Schmidt S, Schachner M. 2003. Region and lamina-specific distribution of extracellular matrix proteoglycans, hyaluronan and tenascin-R in the mouse hippocampal formation. J Chem Neuroanat 26:37–50.

Bruckner G, Szeoke S, Pavlica S, Grosche J, Kacza J. 2006. Axon initial segment ensheathed by extracellular matrix in perineuronal nets. Neuroscience 138:365–375.

Celio MR, Blumcke I. 1994. Perineuronal nets—a specialized form of extracellular matrix in the adult nervous system. Brain Res Brain Res Rev 19:128–145.

Celio MR, Chiquet-Ehrismann R. 1993. 'Perineuronal nets' around cortical interneurons expressing parvalbumin are rich in tenascin. Neurosci Lett 162:137–140.

Celio MR, Spreafico R, De Biasi S, Vitellaro-Zuccarello L. 1998. Perineuronal nets: past and present. Trends Neurosci 21:510–515.

Cohen-Tannoudji M, Babinet C, Wassef M. 1994. Early determination of a mouse somatosensory cortex marker. Nature 368:460–463.

Cooper NG, Steindler DA. 1986a. Monoclonal antibody to glial fibrillary acidic protein reveals a parcellation of individual barrels in the early postnatal mouse somatosensory cortex. Brain Res 380:341–348.

Cooper NG, Steindler DA. 1986b. Lectins demarcate the barrel subfield in the somatosensory cortex of the early postnatal mouse. J Comp Neurol 249:157–169.

Daw MI, Scott HL, Isaac JT. 2007. Developmental synaptic plasticity at the thalamocortical input to barrel cortex: mechanisms and roles. Molecular and cellular neurosciences 34:493–502.

Dawson DR, Killackey HP. 1985. Distinguishing topography and somatotopy in the thalamocortical projections of the developing rat. Brain Res 349:309–313.

Dawson DR, Killackey HP. 1987. The organization and mutability of the forepaw and hindpaw representations in the somatosensory cortex of the neonatal rat. J Comp Neurol 256:246–256.

Deepa SS, Carulli D, Galtrey C, Rhodes K, Fukuda J, Mikami T, Sugahara K, Fawcett JW. 2006. Composition of perineuronal net extracellular matrix in rat brain: a different disaccharide composition for the net-associated proteoglycans. J Biol Chem 281:17789–17800.

Derouiche A, Hartig W, Brauer K, Bruckner G. 1996. Spatial relationship of lectin-labelled extracellular matrix and glutamine synthetase-immunoreactive astrocytes in rat cortical forebrain regions. J Anat 189(Pt 2):363–372.

Dityatev A, Schachner M. 2003. Extracellular matrix molecules and synaptic plasticity. Nat Rev Neurosci 4:456–468.

Elston GN, DeFelipe J, Arellano JI, Gonzilez-Albo MC, Rosa MG. 1999. Variation in the spatial relationship between parvalbumin immunoreactive interneurones and pyramidal neurones in rat somatosensory cortex. Neuroreport 10:975–2979.

Faissner A, Steindler D. 1995. Boundaries and inhibitory molecules in developing neural tissues. Glia 13:233–254.

Ferezou I, Haiss F, Gentet LJ, Aronoff R, Weber B, Petersen CC. 2007. Spatiotemporal dynamics of cortical sensorimotor integration in behaving mice. Neuron 56:907–923.

Freire MA, Gomes-Leal W, Carvalho WA, Guimaraes JS, Franca JG, Picanco-Diniz CW, Pereira A Jr. 2004. A morphometric study of the progressive changes on NADPH diaphorase activity in the developing rat's barrel field. Neurosci Res 50:55–66.

Fuchs JL, Salazar E. 1998. Effects of whisker trimming on GABA(A) receptor binding in the barrel cortex of developing and adult rats. J Comp Neurol 395:209–216.

Fukuda T, Kosaka T, Singer W, Galuske RAW. 2006. Gap junctions among dendrites of cortical GABAergic neurons establish a dense and widespread intercolumnar network. J Neurosci 26:3434–3443.

Galtrey CM, Fawcett JW. 2007. The role of chondroitin sulfate proteoglycans in regeneration and plasticity in the central nervous system. Brain Res Rev 54:1–18.

Geisert E, Bidanset D. 1993. A central nervous system keratan sulfate proteoglycan: localization to boundaries in the neonatal rat brain. Brain Res Dev Brain Res 75:163–173.

Guillery RW. 2002. On counting and counting errors. J Comp Neurol 447:1–7.

Guillery RW, Herrup K. 1997. Quantification without pontification: choosing a method for counting objects in sectioned tissues. J Comp Neurol 386:2–7.

Hartig W, Brauer K, Bruckner G. 1992. Wisteria floribunda agglutinin-labelled nets surround parvalbumin-containing neurons. Neuroreport 3:869–872.

Hausen D, Brückner G, Drlicek M, Härtig W, Brauer K, Bigl V. 1996. Pyramidal cells ensheathed by perineuronal nets in human motor and somatosensory cortex. Neuroreport 7:1725–1729.

Hendry SH, Jones EG, Hockfield S, McKay RD. 1988. Neuronal populations stained with the monoclonal antibody Cat-301 in the mammalian cerebral cortex and thalamus. J Neurosci 8:518–542.

Herndon ME, Lander AD. 1990. A diverse set of developmentally regulated proteoglycans is expressed in the rat central nervous system. Neuron 4:949–961.

Howard CV, Reed M. 2005. Unbiased stereology: three-dimensional measurement in microscopy. Jones C, editor. New York: BIO Scientific.

Inan M, Crair MC. 2007. Development of cortical maps: perspectives from the barrel cortex. Neuroscientist 13:49–61.

Inan M, Lu H-C, Albright MJ, She W-C, Crair MC. 2006. Barrel map development relies on protein kinase a regulatory subunit IIbeta-mediated cAMP signaling. J Neurosci 26:4338–4349.

Innocenti GM, Price DJ. 2005. Exuberance in the development of cortical networks. Nat Rev Neurosci 6:955–965.

Ivy GO, Akers RM, Killackey HP. 1979. Differential distribution of callosal projection neurons in the neonatal and adult rat. Brain Res 173:532–537.

Jhaveri S, Erzurumlu RS, Crossin K. 1991. Barrel construction in rodent neocortex: role of thalamic afferents versus extracellular matrix molecules. Proc Natl Acad Sci U S A 88:4489–4493.

John N, Krugel H, Frischknecht R, Smalla KH, Schultz C, Kreutz MR, Gundelfinger ED, Seidenbecher CI. 2006. Brevican-containing perineuronal nets of extracellular matrix in dissociated hippocampal primary cultures. Mol Cell Neurosci 31:774–784.

Kaas JH, Qi HX, Burish MJ, Gharbawie OA, Onifer SM, Massey JM. 2008. Cortical and subcortical plasticity in the brains of humans, primates, and rats after damage to sensory afferents in the dorsal columns of the spinal cord. Exp Neurol 209:407–416.

Katz LC, Shatz CJ. 1996. Synaptic activity and the construction of cortical circuits. Science 274:1133–1138.

Koppe G, Bruckner G, Brauer K, Hartig W, Bigl V. 1997. Developmental patterns of proteoglycan-containing extracellular matrix in perineuronal nets and neuropil of the postnatal rat brain. Cell Tissue Res 288:33–41.

Koralek KA, Jensen KF, Killackey HP. 1988. Evidence for two complementary patterns of thalamic input to the rat somatosensory cortex. Brain Res 463:346–351.

Kosaka T, Heizmann CW. 1989. Selective staining of a population of parvalbumin-containing GABAergic neurons in the rat cerebral cortex by lectins with specific affinity for terminal N-acetylgalactosamine. Brain Res 483:158–163.

Land PW, Simons DJ. 1985. Cytochrome oxidase staining in the rat SmI barrel cortex. J Comp Neurol 238:225–235.

Massey JM, Hubscher CH, Wagoner MR, Decker JA, Amps J, Silver J, Onifer SM. 2006. Chondroitinase ABC digestion of the perineuronal net promotes functional collateral sprouting in the cuneate nucleus after cervical spinal cord injury. J Neurosci 26:4406–4414.

McRae PA, Rocco MM, Kelly G, Brumberg JC, Matthews RT. 2007. Sensory deprivation alters aggrecan and perineuronal net expression in the mouse barrel cortex. J Neurosci 27:5405–5413.

Mulligan KA, van Brederode JF, Hendrickson AE. 1989. The lectin Vicia villosa labels a distinct subset of GABAergic cells in macaque visual cortex. Vis Neurosci 2:63–72.

Nakagawa F, Schulte BA, Wu SJY, Spicer S. 1986. GABAergic neurons of rodent brain correspond partially with those staining for glycoconjugate with terminal N-acetylgalactosamine. J Neurocytol 15:389–396.

Ohyama J, Ojima H. 1997. Labeling of pyramidal and nonpyramidal neurons with lectin Vicia villosa during postnatal development of the guinea pig. J Comp Neurol 389:453–468.

Ojima H, Kuroda M, Ohyama J, Kishi K. 1995. Two classes of cortical neurones labelled with Vicia villosa lectin in the guinea-pig. Neuroreport 6:617–620.

Olavarria J, Van Sluyters RC, Killackey HP. 1984. Evidence for the complementary organization of callosal and thalamic connections within rat somatosensory cortex. Brain Res 291:364–368.

Oohira A, Matsui F, Watanabe E, Kushima Y, Maeda N. 1994. Developmentally regulated expression of a brain specific species of chondroitin

sulfate proteoglycan, neurocan, identified with a monoclonal antibody IG2 in the rat cerebrum. Neuroscience 60:145–157.

Pereira A Jr, Freire M-AM, Bahia CP, Franca JG, Picanco-Diniz CW. 2000. The barrel field of the adult mouse Sml cortex as revealed by NADPH-diaphorase histochemistry. Neuroreport 11:1889–1892.

Petersen CC. 2007. The functional organization of the barrel cortex. Neuron 56:339–355.

Pizzorusso T, Medini P, Berardi N, Chierzi S, Fawcett JW, Maffei L. 2002. Reactivation of ocular dominance plasticity in the adult visual cortex. Science 298:1248–1251.

Pizzorusso T, Medini P, Landi S, Baldini S, Berardi N, Maffei L. 2006. Structural and functional recovery from early monocular deprivation in adult rats. Proc Natl Acad Sci U S A 103:8517–8522.

Rauch U. 1997. Modeling an extracellular environment for axonal pathfinding and fasciculation in the central nervous system. Cell Tissue Res 290:349–356.

Rice FL. 1985. Gradual changes in the structure of the barrels during maturation of the primary somatosensory cortex in the rat. J Comp Neurol 236:496–503.

Rice F. 1995. Comparative aspects of barrel structure and development. In: Jones EG, Diamond IT, editors. The barrel cortex of rodents. New York: Plenum Press. p 1–62.

Rice FL, Gomez C, Barstow C, Burnet A, Sands P. 1985. A comparative analysis of the development of the primary somatosensory cortex: interspecies similarities during barrel and laminar development. J Comp Neurol 236:477–495.

Riggs GH, Schweitzer L. 1994. Changing patterns of peanut agglutinin labelling in the dorsal cochlear nucleus correspond to axonal ingrowth. J Anat 185(Pt 2):387–396.

Rosen GD, Windzio H, Galaburda AM. 2001. Unilateral induced neocortical malformation and the formation of ipsilateral and contralateral barrel fields. Neuroscience 103:931–939.

Ruoslahti E. 1996. Brain extracellular matrix. Glycobiology 6:489–492.

Schierloh A, Eder M, Zieglgansberger W, Dodt HU. 2004. Effects of sensory deprivation on columnar organization of neuronal circuits in the rat barrel cortex. Eur J Neurosci 20:1118–1124.

Schweizer M, Streit WJ, Muller CM. 1993. Postnatal development and localization of an N-acetylgalactosamine containing glycoconjugate associated with nonpyramidal neurons in cat visual cortex. J Comp Neurol 329:313–327.

Seidenbecher CI, Richter K, Rauch U, Fassler R, Garner CC, Gundelfinger ED. 1995. Brevican, a chondroitin sulfate proteoglycan of rat brain, occurs as secreted and cell surface glycosylphosphatidylinositol-anchored isoforms. J Biol Chem 270:27206–27212.

Seidenbecher CI, Gundelfinger ED, Bockers TM, Trotter J, Kreutz MR. 1998. Transcripts for secreted and GPI-anchored brevican are differentially distributed in rat brain. Eur J Neurosci 10:1621–1630.

Shu SY, Ju G, Fan LZ. 1988. The glucose oxidase-DAB-nickel method in peroxidase histochemistry of the nervous system. Neurosci Lett 85: 169–171.

Steindler DA. 1993. Glial boundaries in the developing nervous system. Annu Rev Neurosci 16:445–470.

Steindler DA, Cooper NG, Faissner A, Schachner M. 1989. Boundaries defined by adhesion molecules during development of the cerebral cortex: the J1/tenascin glycoprotein in the mouse somatosensory cortical barrel field. Dev Biol 131:243–260.

Tollefsen SE, Kornfeld R. 1983. The B4 lectin from Vicia villosa seeds interacts with N-acetylgalactosamine residues alpha-linked to serine or threonine residues in cell surface glycoproteins. J Biol Chem 258: 5172–5176.

Tollefsen S, Kornfeld R. 1987. Vicia villosa lectins. Methods Enzymol 138:536–544.

Uziel D, Garcez P, Lent R, Peuckert C, Niehage R, Weth F, Bolz J. 2006. Connecting thalamus and cortex: the role of ephrins. Anat Rec A Discov Mol Cell Evol Biol 288:135–142.

Van der Loos H, Woolsey TA. 1973. Somatosensory cortex: structural alterations following early injury to sense organs. Science 179:395–398.

Viggiano D. 2000. The two faces of perineuronal nets. Neuroreport 11: 2087–2090.

Wallace MN. 1987. Histochemical demonstration of sensory maps in the rat and mouse cerebral cortex. Brain Res 418:178–182.

Watanabe E, Aono S, Matsui F, Yamada Y, Naruse I, Oohira A. 1995. Distribution of a brain-specific proteoglycan, neurocan, and the corresponding mRNA during the formation of barrels in the rat somatosensory cortex. Eur J Neurosci 7:547–554.

Welker C. 1971. Microelectrode delineation of fine grain somatotopic organization of (SmI) cerebral neocortex in albino rat. Brain Res 26:259–275.

Welker C. 1976. Receptive fields of barrels in the somatosensory neocortex of the rat. J Comp Neurol 166:173–189.

Welker E, Van der Loos H. 1986. Quantitative correlation between barrel-field size and the sensory innervation of the whiskerpad: a comparative study in six strains of mice bred for different patterns of mystacial vibrissae. J Neurosci 6:3355–3373.

Welker C, Woolsey TA. 1974. Structure of layer IV in the somatosensory neocortex of the rat: description and comparison with the mouse. J Comp Neurol 158:437–453.

Wintergerst ES, Faissner A, Celio MR. 1996. The proteoglycan DSD-1-PG occurs in perineuronal nets around parvalbumin-immunoreactive interneurons of the rat cerebral cortex. Int J Dev Neurosci 14:249–255.

Wong-Riley M. 1979. Changes in the visual system of monocularly sutured or enucleated cats demonstrable with cytochrome oxidase histochemistry. Brain Res 171:11–28.

Wong-Riley M, Welt C. 1980. Histochemical changes in cytochrome oxidase of cortical barrels after vibrissal removal in neonatal and adult mice. Proc Natl Acad Sci U S A 77:2333–2337.

Woolsey TA, Van der Loos H. 1970. The structural organization of layer IV in the somatosensory region (SI) of mouse cerebral cortex. The description of a cortical field composed of discrete cytoarchitectonic units. Brain Res 17:205–242.

Yamaguchi Y. 2000. Lecticans: organizers of the brain extracellular matrix. Cell Mol Life Sci 57:276–289.